«Numerical Simulation of the Static Response of Coated Microbubbles: Estimation of Elastic Properties and Comparison with Experiments»

A. Lytra[1], V. Sboros[2], A. Giannakopoulos[3] & N. Pelekasis[1]

[1]University of Thessaly, Department of Mechanical Engineering, Greece.
[2]Herriot Watt University, Institute of Biological Chemistry, UK.
[3]National Technical University of Athens, School of Applied Mathematics & Mechanics, Greece.

Outline

- Introduction
- Mathematical Modeling
- Results
  - Parametric study
  - Comparison with Experiments
- Conclusions

Motivation

- Elastic coating (Polymer or Lipid)
- Initial Diameter ~ 2-5 μm
- Initial Thickness ~ 1-30 nm
- Strong Backscattered Acoustic Signal
- Biocompatibility

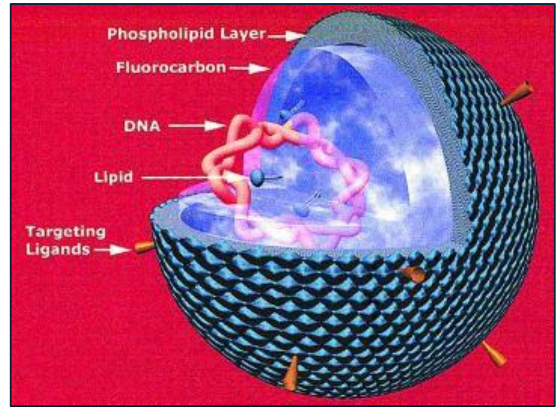

- ➢ Medical Imaging-Diagnostic Applications (Heart, Kidney, Liver)

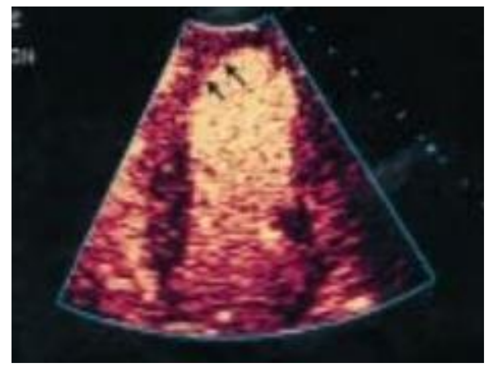

[Blomley et al., *Br. Med. J.*, 2001]
[Song et al., *IEEE Ultrasonics*, 2018]

- ➢ Treatment with microbubbles-Drug or gene delivery

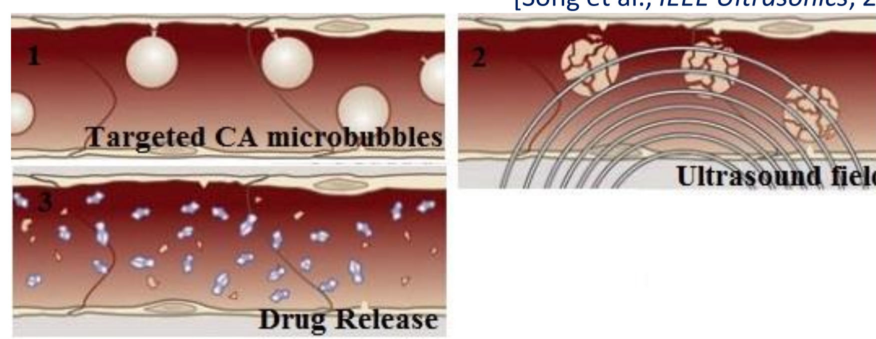

[Ferrara et al., *Annu. Rev. Biomed. Eng.*, 2007]
[Kotopoulis et al., *Med. Physics*, 2013]

Atomic Force Microscope (AFM) Experiments

Microbubbles covered with polymer

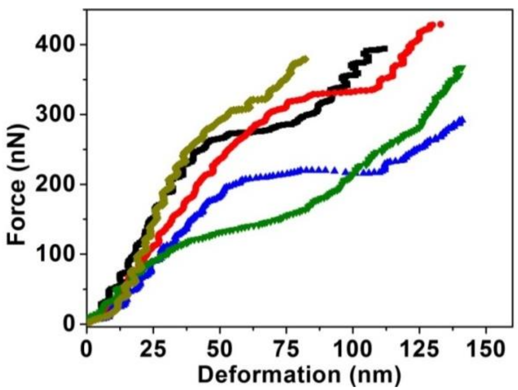

[Glynos et al., *Langmuir*, 2009]

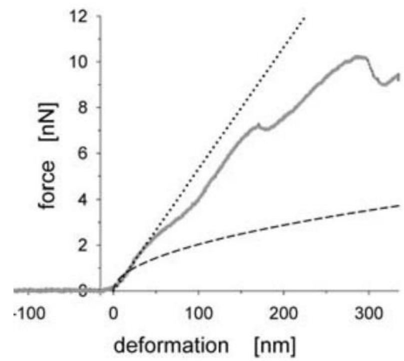

[Elsner et al., *Prog. Col. Pol. Sc.*, 2006]

Microcapsules

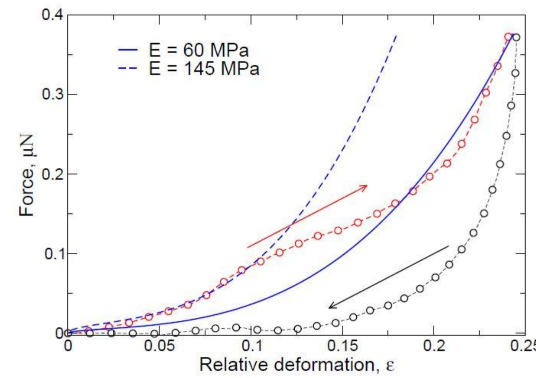

[Lulevich et al., *J. Chem. Phys.*, 2004]

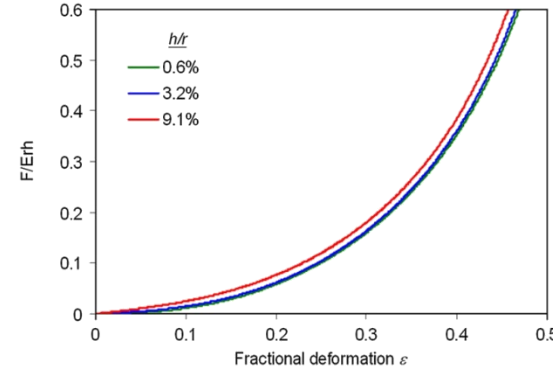

[Mercadé-Prieto et al., *Chem. Eng. Sc.*, 2011]

Microbubbles covered with lipid

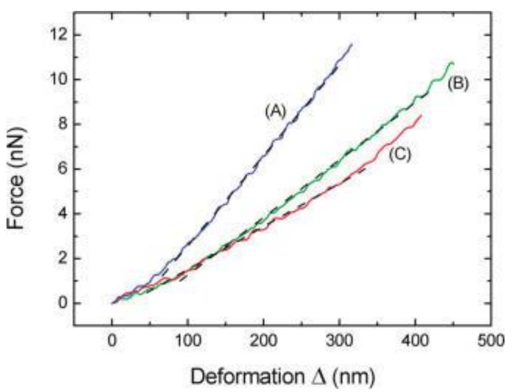

[Bucher-Santos et al., *Langmuir*, 2012]

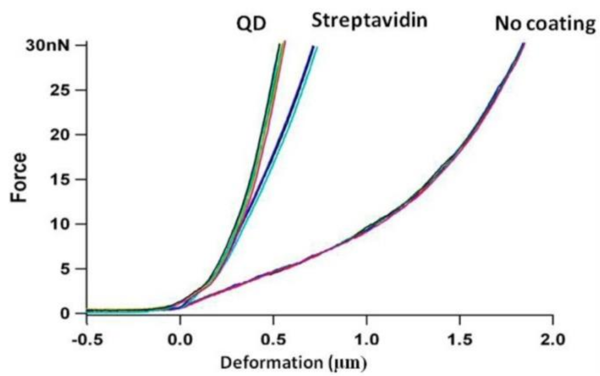

[Abou-Saleh et al., *Langmuir*, 2013]

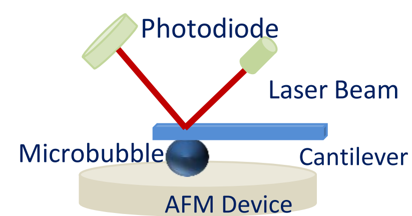

Adhesive Potential-Bubble Covered With Elastic Shell

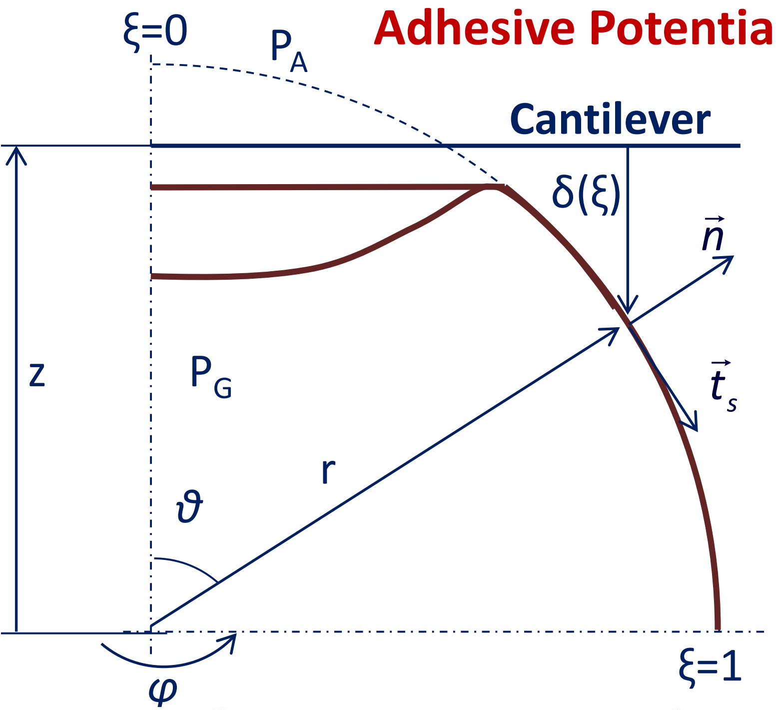

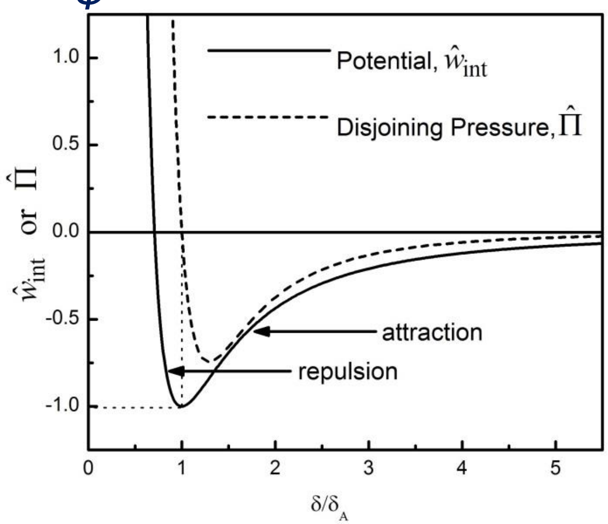

$$\hat{w}_{\rm int} = \frac{w_{\rm int}}{w_0};\ \hat{\Pi} = \frac{\Pi\delta_A}{w_0};\ \Pi = -\frac{\partial w_{\rm int}}{\partial n}$$

$$w_{\rm int}(\delta) = w_o\left[\left(\frac{\delta_A}{\delta}\right)^4 - 2\left(\frac{\delta_A}{\delta}\right)^2\right]$$

repulsion ↑ ↑ attraction

Minimization of energy: $\dfrac{\delta\int W_{\rm int}\,dA}{\delta\vec{r}}$

Normal and Tangential Force Balance

$$P_G - P_A = k_s\tau_{ss} + k_\varphi\tau_{\varphi\varphi} - \frac{1}{\sigma}\frac{\partial(\sigma q)}{\partial s} + 2k_m\left(\gamma_{BW} + w_{\rm int}\right) + \frac{\partial W}{\partial n}$$

$$-\left[\frac{\partial\tau_{ss}}{\partial s} + \frac{1}{\sigma}\frac{\partial\sigma}{\partial s}\left(\tau_{ss} - \tau_{\varphi\varphi}\right) + k_s q\right] = 0, \text{ where } q = \frac{1}{\sigma}\frac{\partial\sigma}{\partial s}\left[\frac{\partial(\sigma m_{ss})}{\partial\sigma} - m_{\varphi\varphi}\right]$$

Isothermal Gas Compression *or* **Constant Volume**

$$P_{G0}V_0^\gamma = P_G V^\gamma \qquad V = V_0$$

Boundary Conditions

$$r_\xi = \vartheta_{\xi\xi} = 0 \text{ at } \xi = 0 \text{ and } 1$$

$$\vartheta = 0 \text{ at } \xi = 0,\ \vartheta = \frac{\pi}{2} \text{ at } \xi = 1$$

Total Force

$$F = \int_A\left(-\frac{\partial w_{\rm int}}{\partial n} - 2k_m w_{\rm int}\right)dA$$

Dimensionless numbers

$$\hat{k}_b = \frac{k_b}{\chi R_o^2};\ \hat{P}_A = \frac{P_A R_o}{\chi};\ \hat{\gamma}_{BW} = \frac{\gamma_{BW}}{\chi};\ \hat{W}_0 = \frac{w_0}{\chi}$$

Unknowns:

r(ξ), θ(ξ), P_G

[Blount et al. *Proc. R. Soc. A*, 2013]
[Starov & Verlade, *J. Phys. Condens. Matter*, 2009]
[Lytra & Pelekasis, *Phys. of Fluids*, 2018]

Constitutive laws & Pre-stressed shell

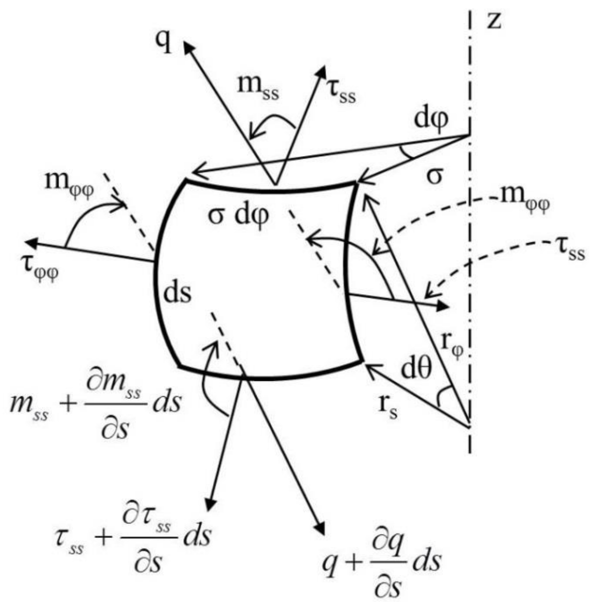

Elastic Tensions

$$\underline{\underline{\tau}} = \frac{2}{J_s}\left[\frac{\partial w}{\partial I_1}\underline{\underline{A}} \cdot \underline{\underline{A}}^T + \frac{\partial w}{\partial I_2} J_s^2 \left(\underline{\underline{I}} - \vec{n}\vec{n}\right)\right]$$

Function of Elastic Energy

$$w^{HK} = \frac{G_s}{4(1-\nu)}\left[\left(\lambda_s^2 - 1\right)^2 + 2\nu\left(\lambda_s^2 - 1\right)\left(\lambda_\varphi^2 - 1\right) + \left(\lambda_\varphi^2 - 1\right)^2\right]$$

$$w^{MR} = w\left(I_1, I_2\right) = \frac{G_{MR}}{2}\left[\left(1-b\right)\left(I_1 + 2 + \frac{1}{I_2 + 1}\right) + b\left(\frac{I_1 + 2}{I_2 + 1} + I_2 + 1\right)\right]$$

$$w^{SK} = w\left(I_1, I_2\right) = \frac{G_{SK}}{4}\left[I_1^2 + 2I_1 - 2I_2 + CI_2^2\right]$$

Function of bending $w_b = \frac{k_b}{2}\left(K_s^2 + 2\nu K_s K_\varphi + K_\varphi^2\right)$

Gas compression: $\hat{w}_c = V\left(P_A + \Delta P + \frac{P_G}{\gamma - 1}\right) - V_o\left(P_A + \frac{P_A + 2\gamma_{BW}}{\gamma - 1}\right)$

Surface energy: $\hat{w}_s = \int_A \gamma_{BW} dA$

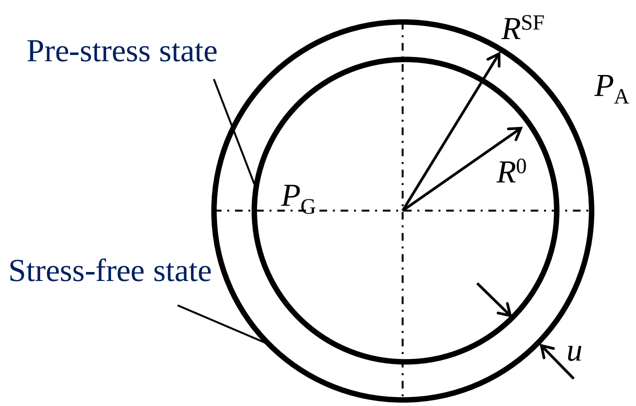

$$R^{SF} = R^0 - u$$

$$\lambda_s = \lambda_\varphi = \frac{R^0}{R^0 - u}$$

$$P_G = P_A + 2\gamma_{BW} + \tau_{ss} + \tau_{\varphi\varphi}$$

[Timoshenko & Woinowsky-Krieger, *Theory of plates and shells*. 1959]
[Barthès-Biesel et al., *J. Fluid Mech.*, 2002]
[Pozrikidis, *Modeling and Simulation of Capsules & Biological Cells* 2003]

Finite Element Method

- **Method of Weighted Residuals:** $\underline{\underline{J}} \cdot d\vec{c} = \vec{R}$ $\underline{\underline{J}}$: Jacobian Matrix

  $\vec{c}$: Uknown coefficients

  $\vec{R}$: Residuals

- **Basis Functions:**
  B-Cubic Splines

$$B_i\left(t_j\right) = \begin{cases} 4, & j = 1 \\ 1, & j = i \pm 1 \\ 0, & j = i \pm 2 \end{cases}$$

- **Solution of the System:** Newton-Raphson Iterations
  Simple or Arc-Length Continuation

Validation

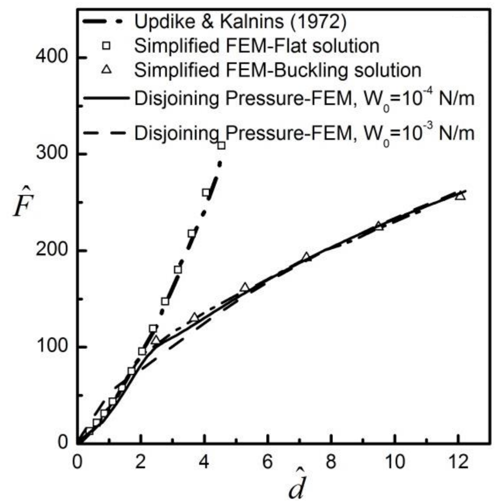

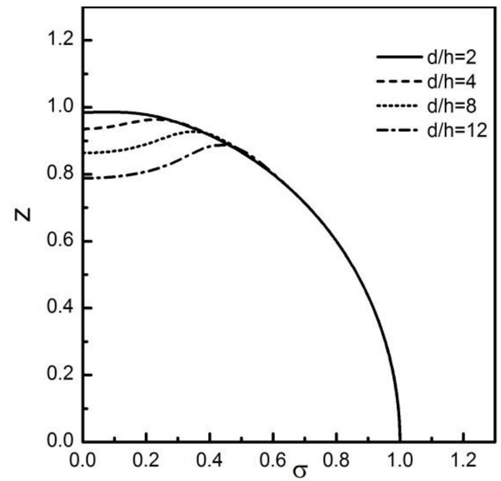

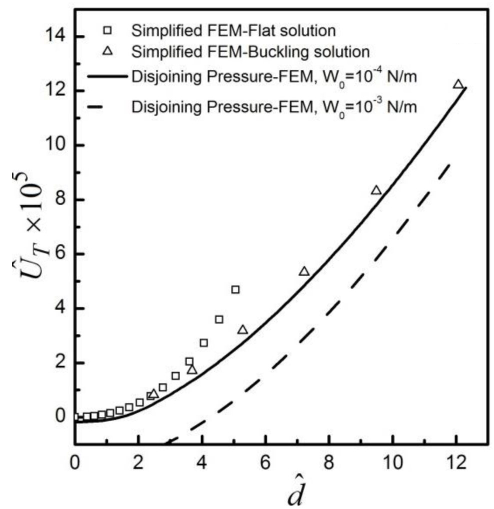

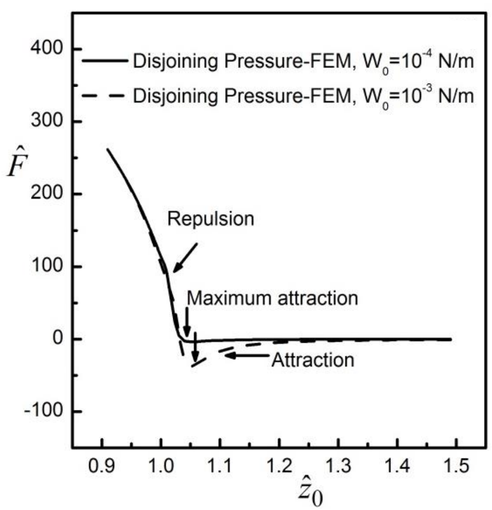

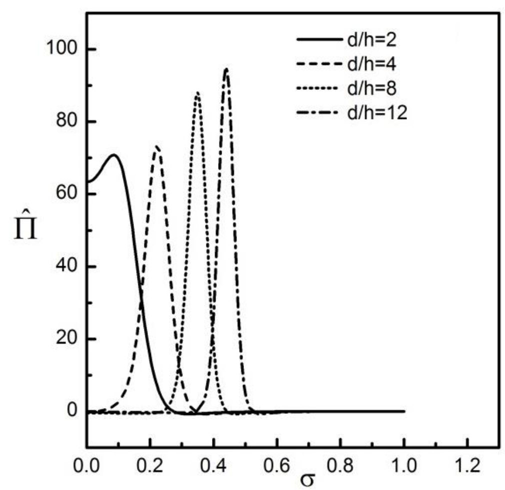

- The numerical model recovers the analytical solution.
- The flat solution after the buckling point is unstable.
- The pick of the disjoining pressure profile is located at the end of contact area for flat shapes and at the dimple for buckled shapes.

$$\hat{k}_b = 9\cdot 10^{-6}, \hat{P}_A = 10^{-2}, \hat{W}_0 = 10^{-4} \textit{ or } 10^{-3}, \hat{\gamma}_{BW} = 0$$
$$E = 10^9 Pa, R/h = 100$$
$$v = 0.3, \gamma = 0, \textit{ Hooke's law}, \mathrm{u} = 0$$

[Updike & Kalnins, *Trans. ASME*, 1970, 1972, 1972]

Asymptotic Solutions

- Linear response in f-d curve with flat shapes

Reissner's eq. $F = \frac{4}{\left[3\left(1-\nu^2\right)\right]^{0.5}} \frac{Eh^2}{R_0} \Delta$ or $F = 8\sqrt{\chi k_b} \frac{\Delta}{R_0}$

- Curved downwards response with buckled shapes

Pogorelov's eq. $F = \left[\frac{3.56 E^2 h^5}{\left(1-\nu^2\right) R_o^2} \Delta \right]^{0.5}$

- Curved upwards response with flat shapes

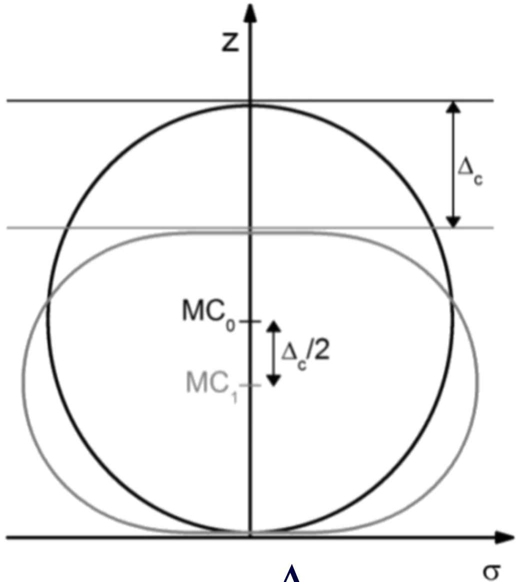

$$\Delta = \frac{\Delta_c}{2}$$

Pressure dominated regime: $F = \frac{4\pi\chi}{R_0^2} \Delta^3 = 4\pi\chi R_0 \left(\frac{\Delta}{R_0} \right)^3$

Total Force: $F = 8\sqrt{\chi k_b} \frac{\Delta}{R_0} + 4\pi\chi R_0 \left(\frac{\Delta}{R_0} \right)^3$

[Reissner, *J. Math. Phys.*, 1946]
[Pogorelov, *Am. Math. Soc.*, 1988]
[Landau, *Theory of Elasticity*, 1986]
[Shanahan, *J. Adhesion*, 1997]
[Lulevich et al. , *J. Chem. Phys.*, 2004]
[Lytra & Pelekasis, *Phys. of Fluids*, 2018]

Parametric Study: $\hat{P}_A << 1$ Microbubbles covered with polymer: ***Effect of bending***

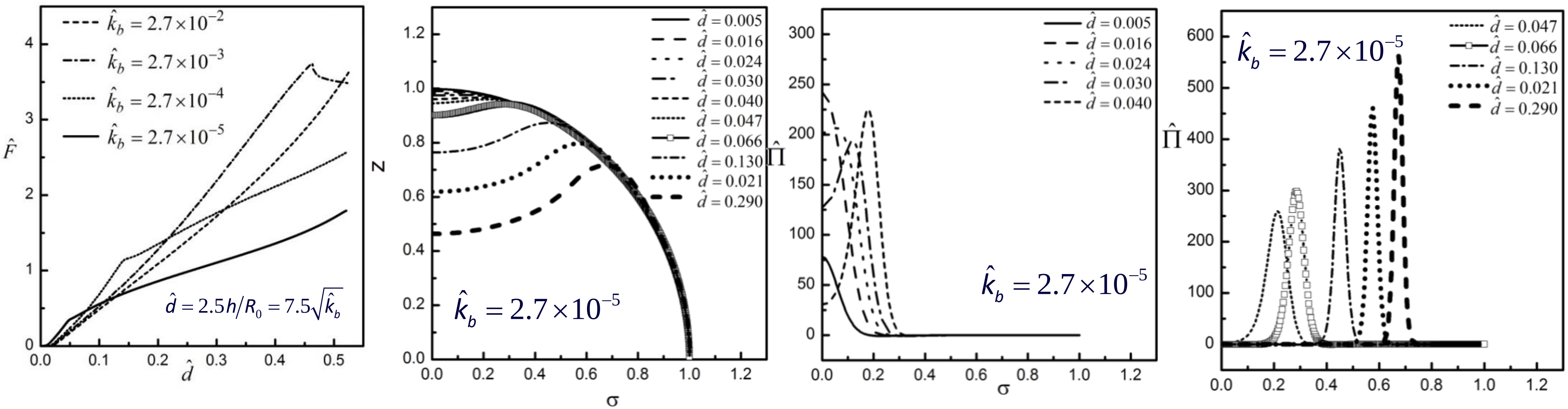

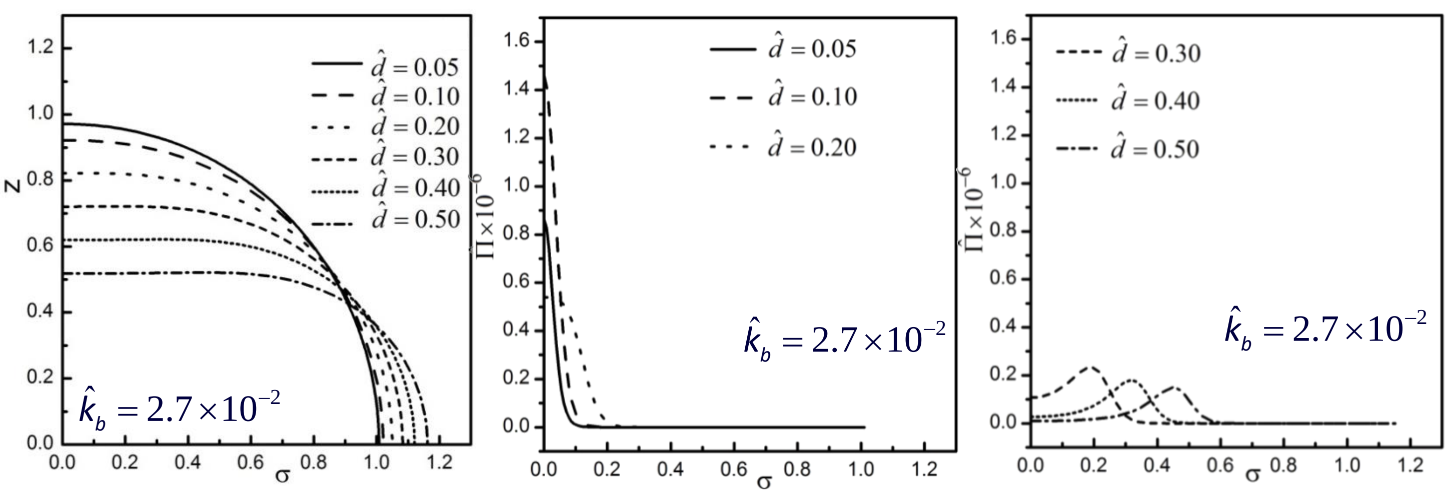

- The f-d curves initially follow the **Reissner** regime and then the **Pogorelov**.
- Increasing bending postpones buckling.
- Disjoining pressure is concentrated around the contact area at small deformations and at the end of contact for higher deformations.

$\hat{P}_A = 3\times10^{-4},\ \hat{W}_0 = 2\times10^{-6},\ \hat{\gamma}_{BW} = 0$
$v = 0.5,\ \gamma = 0,\ \textit{Hooke's law},\ \mathrm{u} = 0$

[Lytra & Pelekasis, *Phys. of Fluids*, 2018]

$\hat{P}_A << 1$ Microbubbles covered with polymer: *Comparison with AFM experiments*

AFM Experiment by *Elsner et al., Prog. Col. Pol. Sc., 2006*

$R_0 = 7.9$ μm, $h = 25$ nm, $E = 252$ MPa, $W_0 = 10^{-5}$ N/m, $v = 0.33$, $\gamma = 1.07$, *Hooke's law*, $\hat{k}_b = 9.4\times10^{-7}$, $\hat{P}_A = 1.3\times10^{-1}$, $\hat{W}_0 = 1.6\times10^{-6}$, $\hat{\gamma}_{BW} = 0$

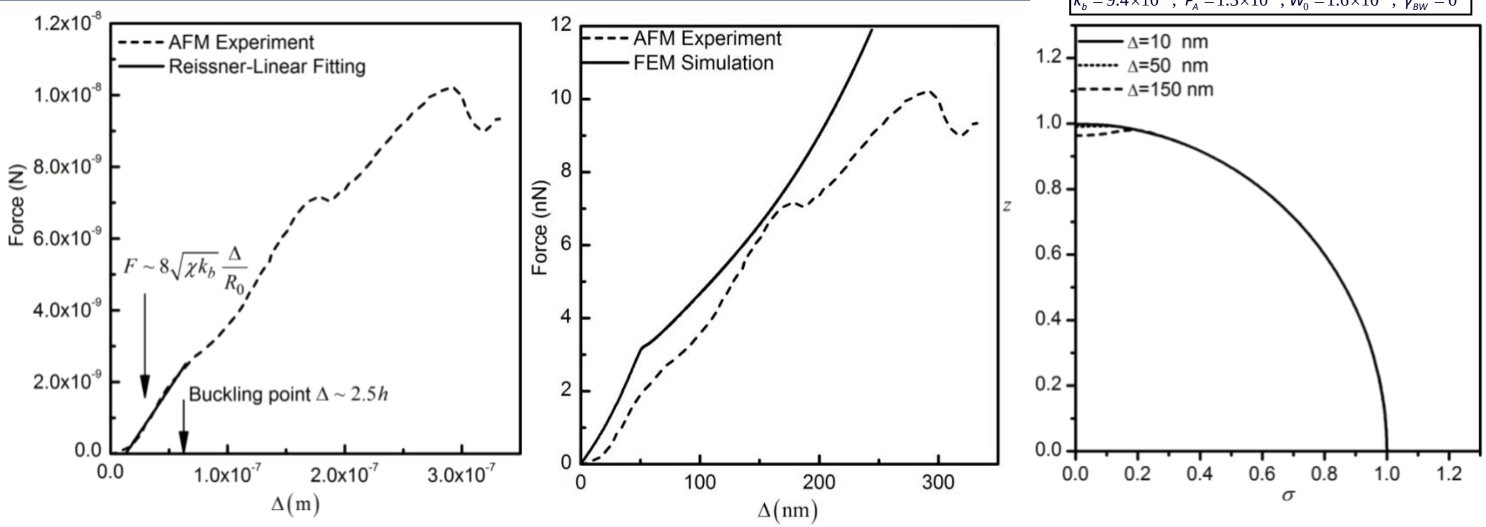

- The f-d curves initially follow the **Reissner**, then the **Pogorelov** & at high deformations the pressure dominate regime.
- Similar response in the AFM experiment with instabilities at higher deformations.
- Coupling of the Reissner's regime and the buckling point estimate the elastic properties.
- Satisfactory agreement between the two curves.

AFM Experiment by *Glynos et al., Langmuir, 2009*

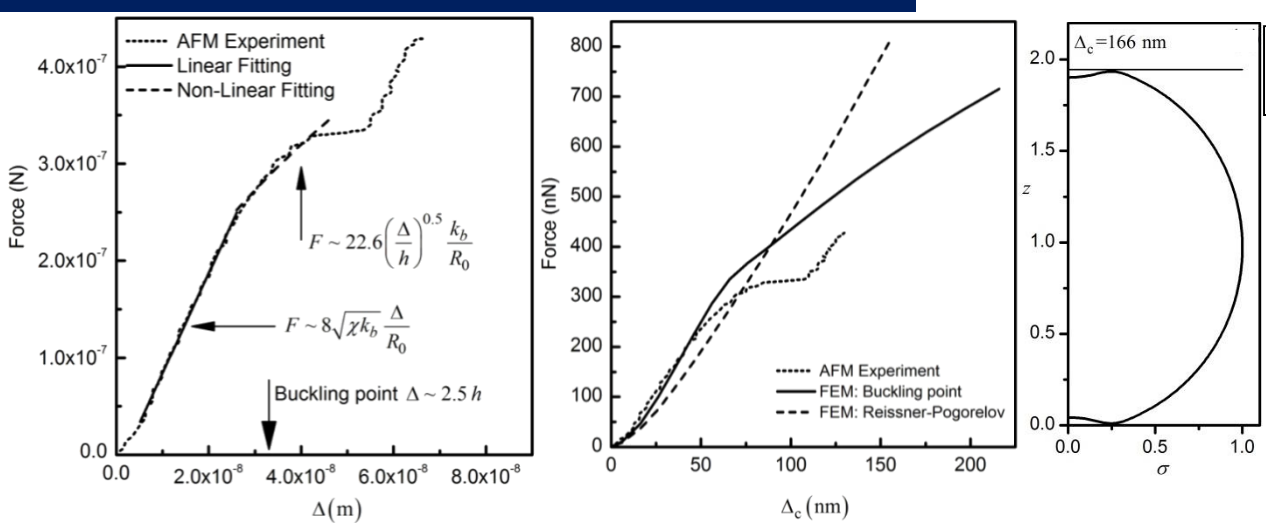

Reissner & Buckling point

$R_0 = 2$ μm, $h = 13$ nm, $E = 48$ GPa, $W_0 = 10^{-3}$ N/m, $v = 0.42$, $\gamma = 1.07$, *Hooke's law*, $\hat{k}_b = 4.3\times10^{-6}$, $\hat{P}_A = 3.2\times10^{-4}$, $\hat{W}_0 = 1.6\times10^{-6}$, $\hat{\gamma}_{BW} = 0$

Reissner to Pogorelov

$h = 36$ nm, $E = 6$ GPa

- Same response pattern in f-d curves.
- The Reissner to Pogorelov transition overestimates the deformation.
- Combination of Reissner model & the buckling point predicts better the experiment.
- The horizontal plateau in experimental curve indicates inelastic effects.

[Lytra et al., *Soft Matter*, submitted]

Comparison with compression experiment for a table tennis ball

Experiment by *Shorter et al., J. Mech. Mat. & Str., 2010*

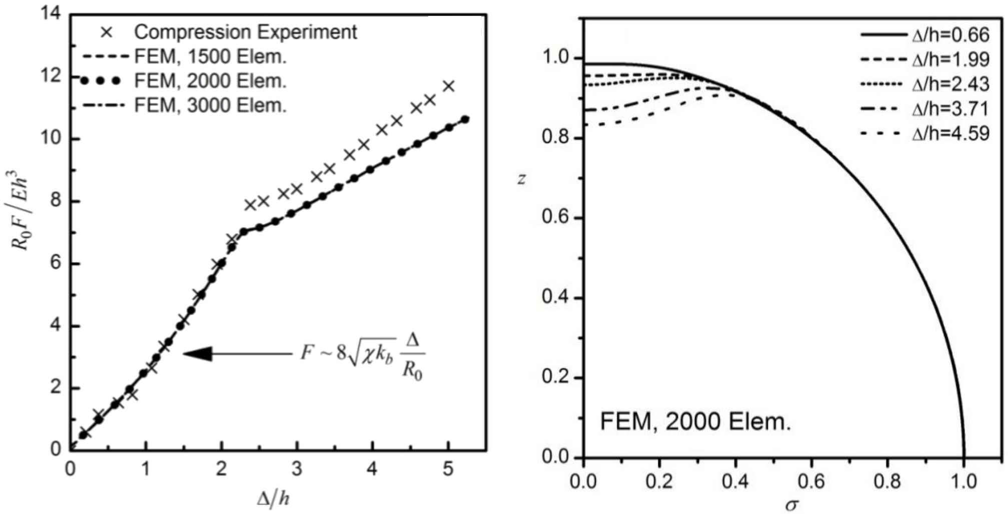

Reissner & Buckling point

$R_0 = 2$ cm, $h = 0.4$ mm,
$E = 2.8$ MPa, $A = 10^{-10}$ Nm,
$v = 0.4$, $\gamma = 0$, *Hooke's law*,
$\hat{k}_b = 4\times10^{-5}$, $\hat{P}_A = 0$,
$\hat{A} = 2.2\times10^{-10}$, $\hat{\gamma}_{BW} = 0$, $u = 0$

- A pure repulsive potential is considered here (Hamaker).
- The transition area between the contact and the outer shell is very small in comparison with the shell radius. Thus an area of high curvature is formed, which requires a finer mesh in order to obtain a converged solution.

[Lytra et al., *Soft Matter*, submitted]

Parametric Study: $\hat{P}_A \sim 1$ Microbubbles covered with phospholipid: ***Effect of bending***

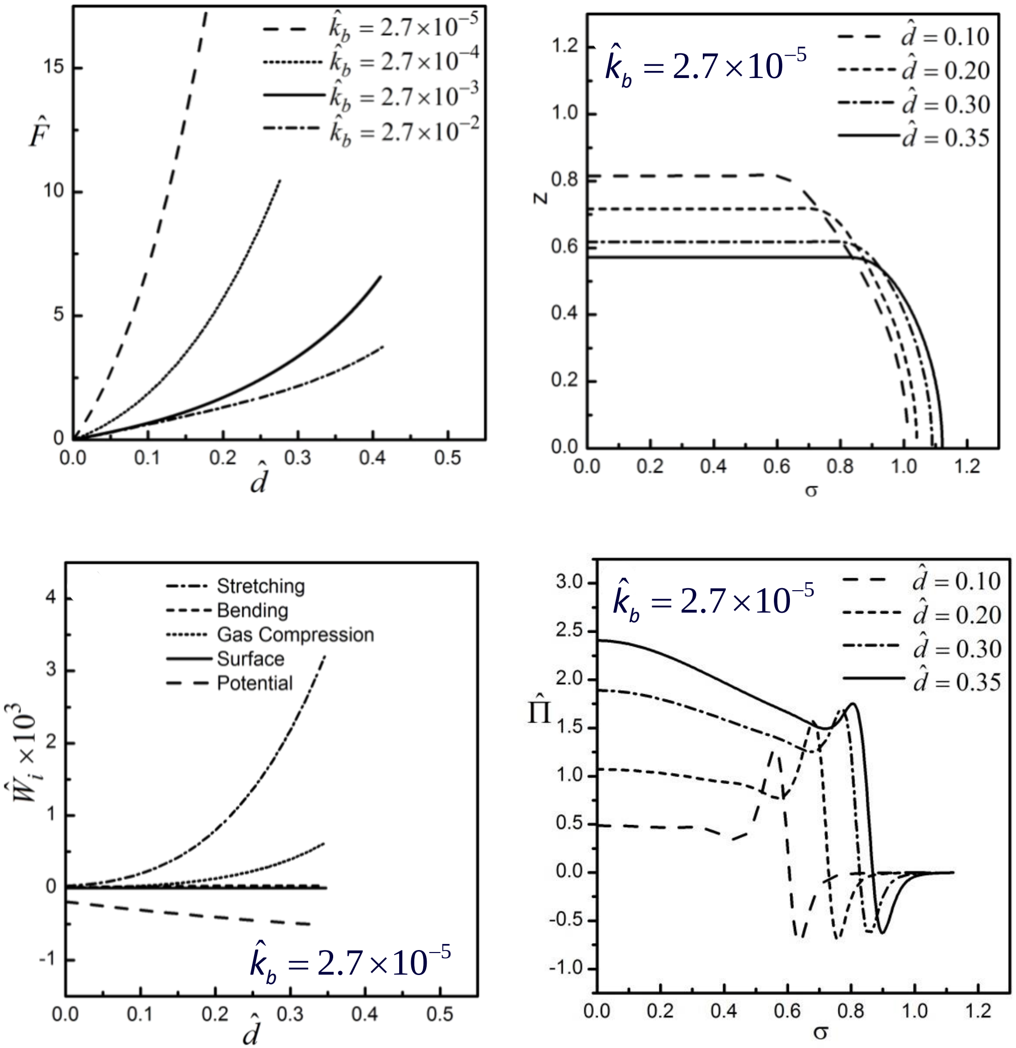

$\hat{P}_A = 3,\ \hat{W}_0 = 2\times10^{-3},\ \hat{\gamma}_{BW} = 0$

$\nu = 0.5,\ \gamma = 0,\ Mooney-Rivlin\ law,\ \mathrm{u} = 0$

- When elasticity is comparable with the gas pressure buckling is by-passed to a curved up-wards regime even for shell with small bending modulus.
- The increase of bending extends the validity of Reissner regime.
- The profiles of the disjoining pressure have a non-zero plateau in the contact area, which is responsible for the cubic dependence of the f-d curve.

[Lytra & Pelekasis, *Phys. of Fluids*, 2018]

$\hat{P}_A \sim 1$ Microbubbles covered with phospholipid: *Comparison with AFM experiments*

Experiment by *Bucher Santos et al., Langmuir, 2012.*

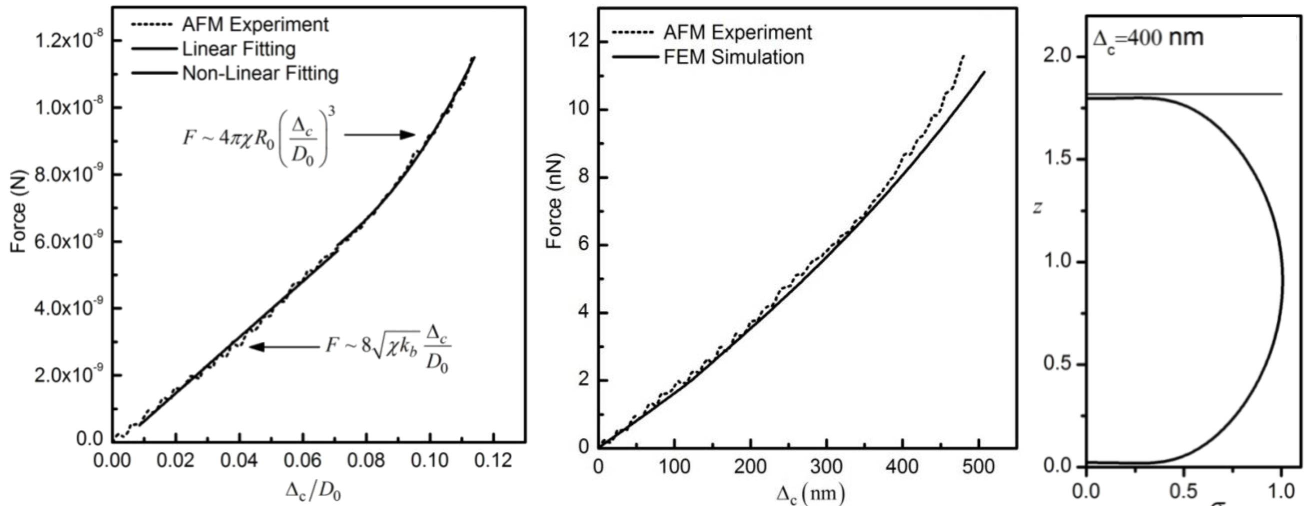

Reissner & pressure dominated regime

$R_0 = 2.1\mu m$, $\chi = 0.19$ N/m, $k_b = 5.8\times10^{-16}$ Nm, $W_0 = 10^{-4}$ N/m,
$\nu = 0.5$, $\gamma = 1.07$, Mooney-Rivlin law,
$\hat{k}_b = 6.9\times10^{-4}$, $\hat{P}_A = 1.1$, $\hat{W}_0 = 5.2\times10^{-4}$, $\hat{\gamma}_{BW} = 0$

- The experimental f-d curve follows the initial linear Reissner's regime and then the curved upwards cubic regime.
- Coupling of the two asymptotic models gives reliable estimates of the area elasticity and bending moduli.
- Numerical and experimental curves are in excellent agreement.
- The MB remains flattened around the contact area even at higher values of deformation.

Experiment by *Abou-Saleh et al., Langmuir, 2013.*

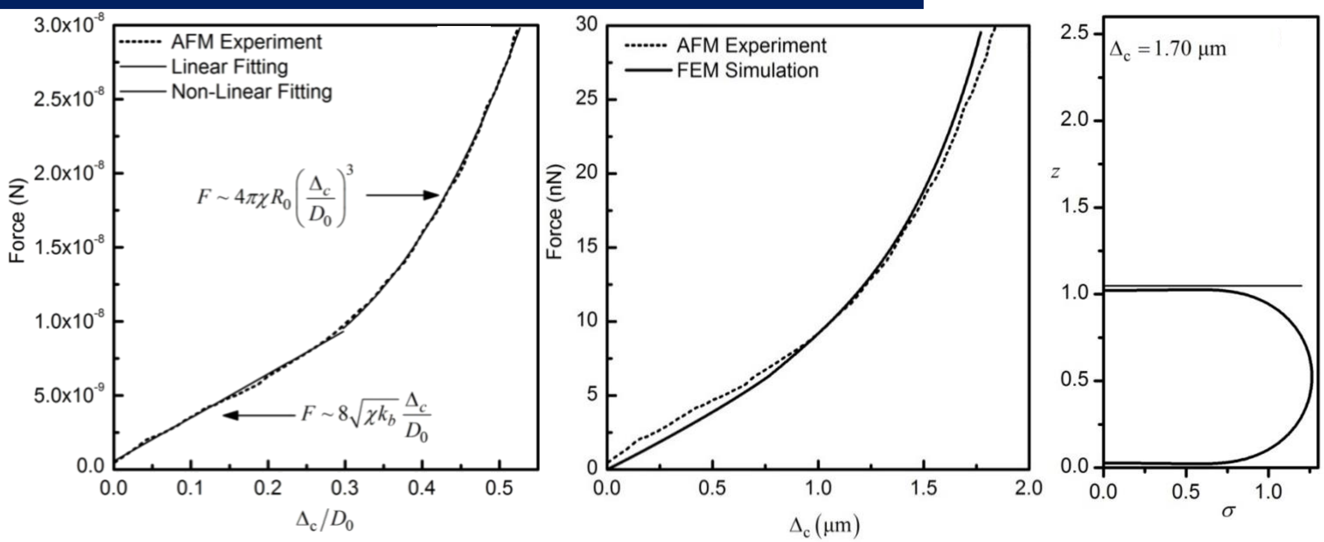

Reissner & pressure dominated regime

$R_0 = 1.75$ μm, $\chi = 7.7\times10^{-3}$ N/m, $k_b = 1.76\times10^{-15}$ Nm, $W_0 = 10^{-4}$ N/m,
$\nu = 0.5$, $\gamma = 1.07$, Mooney-Rivlin law,
$\hat{k}_b = 7.5\times10^{-2}$, $\hat{P}_A = 2.3$, $\hat{W}_0 = 1.3\times10^{-2}$, $\hat{\gamma}_{BW} = 0$

[Lytra et al., *Soft Matter*, submitted]

$\hat{P}_A >> 1$ Capsules with constant volume: <u>*Comparison with AFM experiments*</u>

Experiment by *Lulevich et al., J. Chem. Phys., 2004.-PLA*

$R_0 = 5$ μm, $E = 1$ MPa, $h = 25$ nm, $W_0 = 10^{-5}$ N/m
$v = 0.5$, Hooke's law,
$\hat{k}_b = 2.78\times10^{-6}$, $\hat{P}_A = 20$, $\hat{W}_0 = 4\times10^{-4}$, $\hat{\gamma}_{BW} = 0$

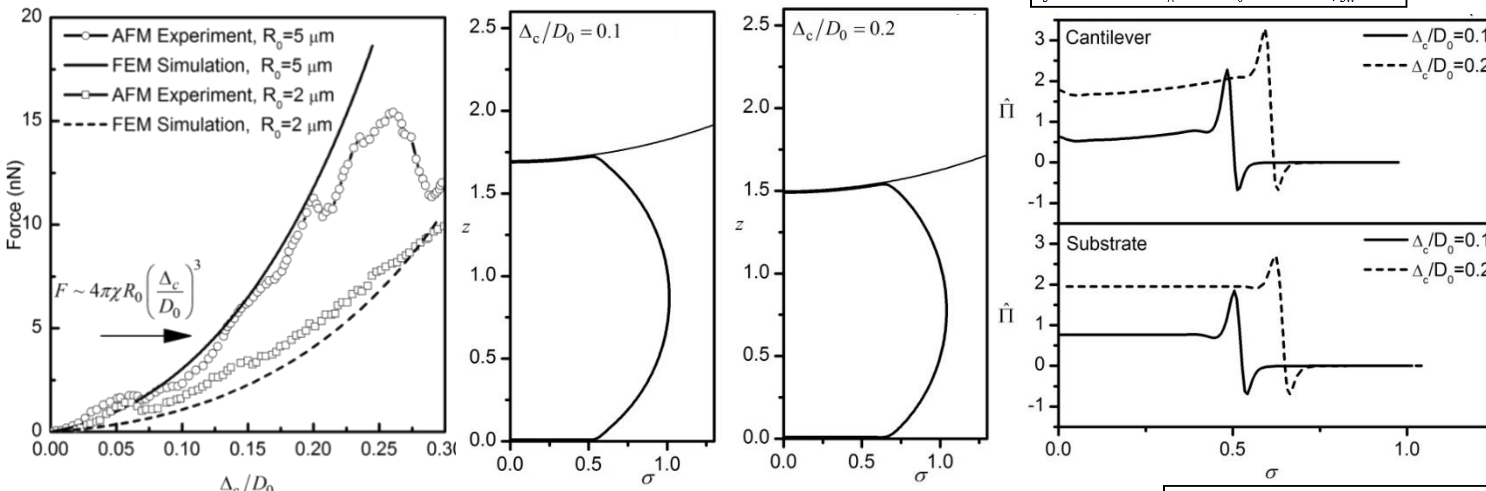

- The experimental f-d curve follows the curved upwards cubic regime.
- The linear regime disappears due to relatively small bending resistance.
- The asymmetric loading conditions do not introduce significant discrepancies.
- Both contact areas remain flattened without buckling.

Experiment by *Mercadé-Prieto et al., Chem. Eng. Sc., 2011.-MF*

$R_0 = 4.4$ μm, $E = 1.17$ GPa, $h = 290$ nm, $W_0 = 10^{-5}$ N/m
$v = 0.5$, Hooke's law,
$\hat{k}_b = 4.8\times10^{-4}$, $\hat{P}_A = 1.3\times10^{-3}$, $\hat{W}_0 = 3\times10^{-8}$, $\hat{\gamma}_{BW} = 0$

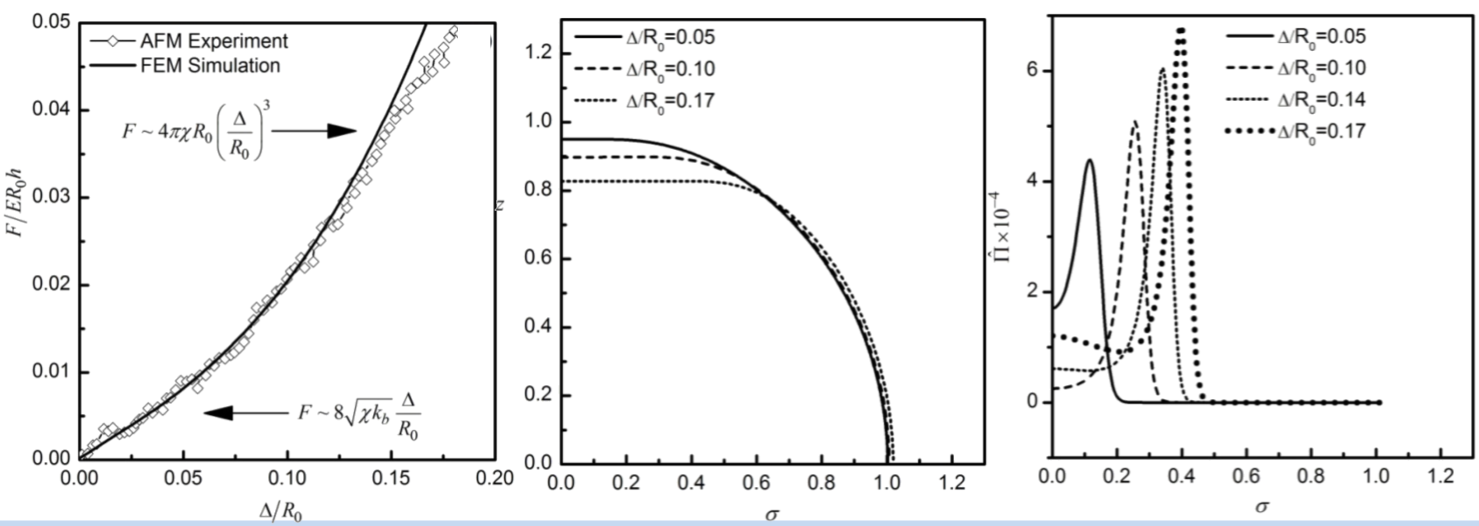

- The experimental f-d curve follows the linear Reissner regime and then the curved upwards cubic regime.
- The disjoining pressure reflect also the calculated f-d curves:
- PLA: constant and increasing disjoining pressure near the contact area even at small values of deformations.
- MF: Initially point load at the end of contact area and then non-zero around the contact for higher deformation.

$\hat{P}_A >> 1$ Capsules with constant volume: *Comparison with AFM type experiments*

Experiment by *Frostad et al.* (on going work…)

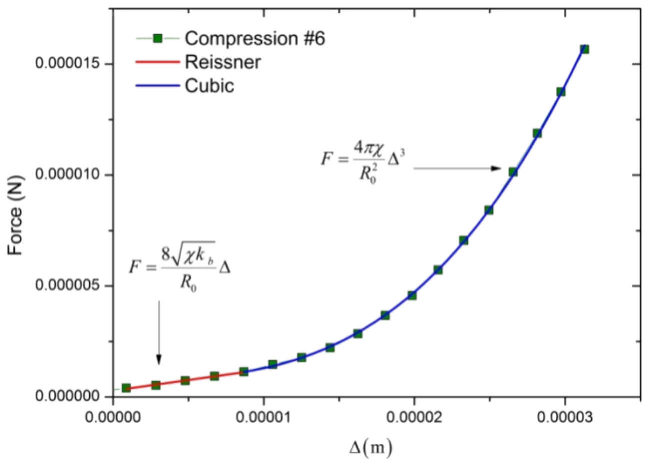

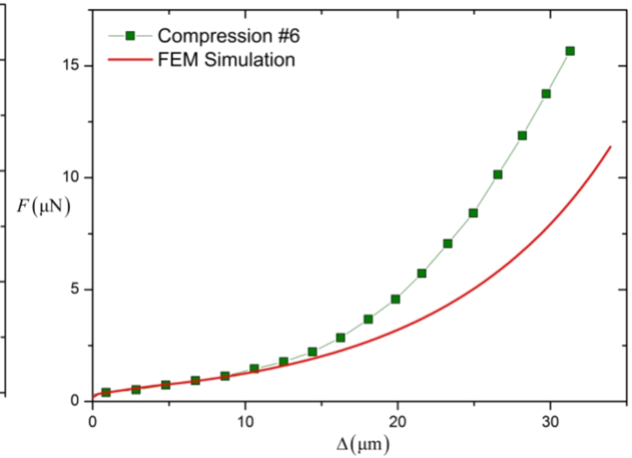

- The experimental f-d curve follows the linear Reissner regime and then the curved upwards cubic regime.
- The numerical curve predicts very well the linear regime, but underestimates the force in the non-linear regime.
- Asymmetric scenarios are investigated.
- Modelling improvement required.

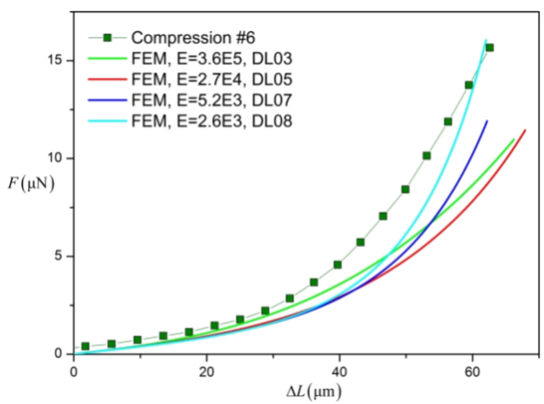

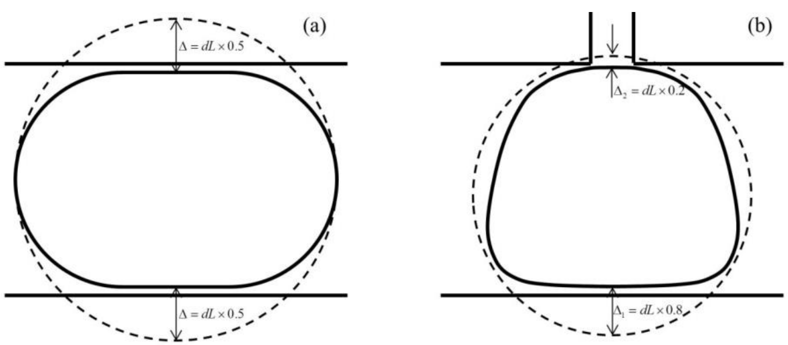

Modelling & Simulations of AFM Experiments

- A theoretical model is presented to simulate afm experiments.

- **MB covered with polymer:** The f-d curve follows the Reissner and then the Pogorelov regime, where buckling takes place.

- **MB covered with lipid:** The f-d curves follow the Reissner and then the pressure dominated regime, where the shape remains flattened in the contact area.

- **Capsules with constant volume:** The f-d curves follow the same response pattern as MB covered with lipid.

  But, for relatively small bending resistance the linear regime shrinks and the cubic response dominates even at low values of deformation.

- The increase of bending postpones buckling.

- Gas pressure prevents buckling even for relatively thin shells.

- The elastic properties can be estimated from the f-d curves for both type of materials, based on simple analytical solutions.

- The theoretical model recovers the experiments for a wide range of afm data.

This work was performed in the framework of the operational program: «Education and lifelong learning» - «**Aristeia**» and was cofounded by the European Union (European Social Fund), national resources

and the **Dep. of Mechanical Engineering-University of Thessaly**.

http://contrast-aristeia.mie.uth.gr/

Thank you for your attention!

European Union
European Social Fund

OPERATIONAL PROGRAMME
EDUCATION AND LIFELONG LEARNING
investing in knowledge society
MINISTRY OF EDUCATION & RELIGIOUS AFFAIRS
MANAGING AUTHORITY
Co-financed by Greece and the European Union

NSRF
2007-2013
programme for development
EUROPEAN SOCIAL FUND

Extra Slides

Asymptotic Analysis for Microbubbles covered with Lipid Monolayer

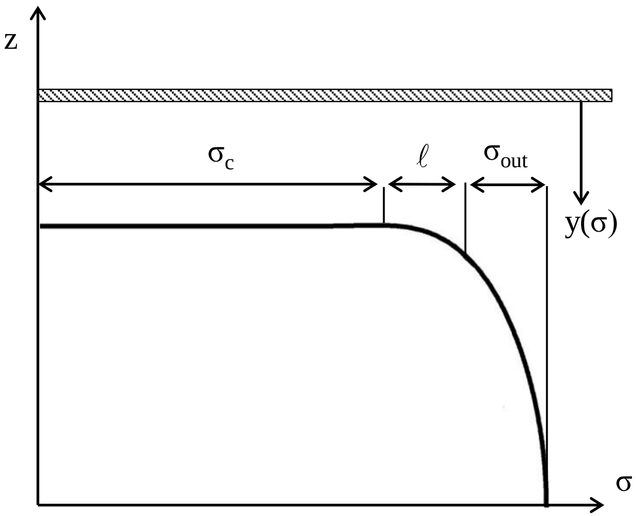

Contact regime (shear vanish)

$$\begin{cases} \vec{n}: P_G - P_A \approx \dfrac{\partial W}{\partial n} \\ \vec{t}_s: \dfrac{\partial \tau_{ss}}{\partial s} \approx -\dfrac{1}{\sigma}\dfrac{\partial \sigma}{\partial s}\left(\tau_{ss} - \tau_{\varphi\varphi}\right) \end{cases}$$

Transition regime (Bending ~ Dis.Pressure)

$$k_b \frac{\delta_A}{\ell^4} \sim \frac{W_0}{\delta_A} \rightarrow \ell \sim \delta_A^{1/2}\left(k_b / W_0\right)^{1/4}$$

$$\rightarrow \ell / R_0 \sim \left(\delta_A / R_0\right)^{1/2}\left(\frac{k_b}{W_0 R_0^2}\right)^{1/4} \rightarrow \ell << R_0$$

$$\begin{cases} \vec{n}: \dfrac{\partial \hat{q}}{\partial \hat{s}} \approx \dfrac{\partial W}{\partial n} \\ \vec{t}_s: \dfrac{\partial \tau_{\hat{s}\hat{s}}}{\partial \hat{s}} \approx -k_s \hat{q} \end{cases} \qquad q = \frac{q'}{k_b\left(1/R_0^2\right)}, \quad \hat{q} = \frac{q'}{k_b\left(\delta_A / \ell^3\right)}$$

$$q = \frac{\partial m_s}{\partial s} + \frac{m_s}{\sigma}\frac{\partial \sigma}{\partial s} - \frac{\partial \sigma}{\partial s}\frac{m_\phi}{\sigma} \xrightarrow{m_s \sim \hat{m}_s} \hat{q} \approx \frac{\partial \hat{m}_s}{\partial \hat{s}}$$

Outer regime

$$\begin{cases} \vec{n}: \left(P_G - P_A\right) = k_s \tau_{ss} + k_\varphi \tau_{\varphi\varphi} - \dfrac{1}{\sigma}\dfrac{\partial\left(\sigma q\right)}{\partial s} + \gamma_{BW}\left(\vec{\nabla}_s \cdot \vec{n}\right) \\ \vec{t}_s: \dfrac{\partial \tau_{ss}}{\partial s} + \dfrac{1}{\sigma}\dfrac{\partial \sigma}{\partial s}\left(\tau_{ss} - \tau_{\varphi\varphi}\right) + k_s q = 0 \end{cases}$$

$$q = \frac{\partial m_s}{\partial s} + \frac{m_s}{\sigma}\frac{\partial \sigma}{\partial s} - \frac{\partial \sigma}{\partial s}\frac{m_\phi}{\sigma}, \qquad P_G V^\gamma = P_{G0} V_0^\gamma$$

Total force

$$F = F_C + F_{Tr} \approx \left(P_G - P_A\right)\pi L^2 + q' 2\pi L$$

Classic Contact Problem

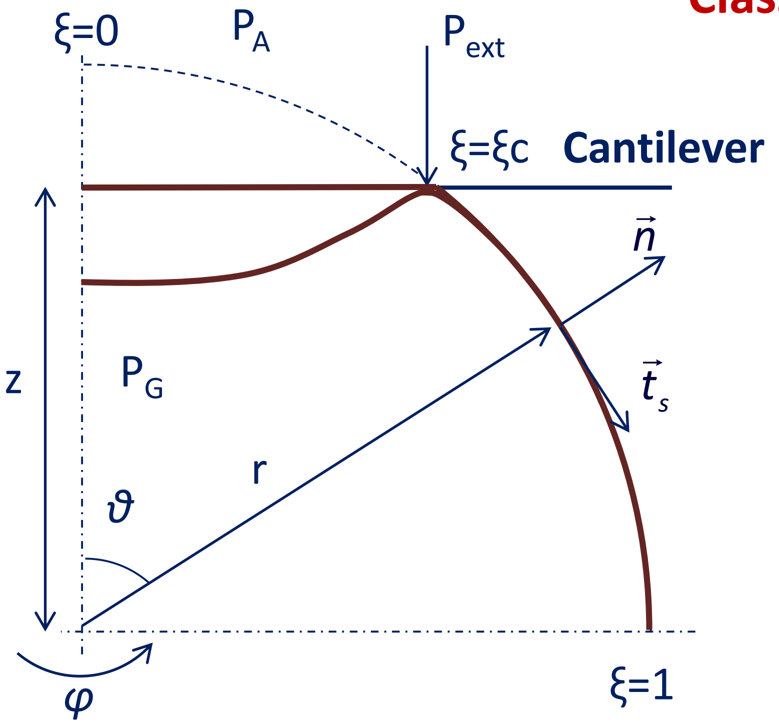

Normal and Tangential Force Balance

$$\Delta\vec{F} = \Delta\vec{P} \Rightarrow \begin{cases} \Delta\vec{F}_N = \left(P_G - P_A - P_{ext}(\xi)\right)\underline{\underline{I}}\cdot\vec{n} \\ \Delta\vec{F}_s = \vec{0} \end{cases}$$

$$\Delta\vec{F} = -\vec{\nabla}_s\cdot\left(\tau_{ss}\vec{t}_s\vec{t}_s + \tau_{\varphi\varphi}\vec{t}_\varphi\vec{t}_\varphi + q\vec{t}_s\vec{n}\right) + \gamma_{BW}\vec{\nabla}_s\cdot\vec{n}$$

$$\vec{q} = \vec{\nabla}_s\cdot\underline{\underline{m}}\cdot\left(\underline{\underline{I}} - \vec{n}\vec{n}\right)$$

$$\begin{cases} \vec{n}: P_G - P_A - P_{ext}(\xi) = k_s\tau_{ss} + k_\varphi\tau_{\varphi\varphi} - \dfrac{1}{\sigma}\dfrac{\partial(\sigma q)}{\partial s} + 2k_m\gamma_{BW} \\ \vec{t}_s: -\left[\dfrac{\partial\tau_{ss}}{\partial s} + \dfrac{1}{\sigma}\dfrac{\partial\sigma}{\partial s}\left(\tau_{ss} - \tau_{\varphi\varphi}\right) + k_s q\right] = 0 \end{cases}$$

$$q = \frac{1}{\sigma}\frac{\partial\sigma}{\partial s}\left[\frac{\partial(\sigma m_{ss})}{\partial\sigma} - m_{\varphi\varphi}\right], P_{ext}(\xi) = \begin{cases} P_{ext}, \xi = \xi_c \\ 0, \ \xi \neq \xi_c \end{cases}$$

Kinematic Condition

$z_\xi = 0$ at $\xi = \xi_c$

Comparison against experiments

↓

Deformation=$R_o - z(\xi_c)$

Isothermal Gas Compression

$$P_{G0}V_0^\gamma = P_G V^\gamma$$

Boundary Conditions

$r_\xi = \vartheta_{\xi\xi} = 0$ at $\xi = 0$ and 1

$\vartheta = 0$ at $\xi = 0$, $\vartheta = \dfrac{\pi}{2}$ at $\xi = 1$

$$\hat{r} = \frac{r}{R_o};\ \hat{k}_b = \frac{k_b}{\chi R_o^2};\ \hat{P}_A = \frac{P_A R_o}{\chi};\ \hat{\gamma}_{BW} = \frac{\gamma_{BW}}{\chi};\ \hat{\chi} = 1$$

$$\boxed{\hat{k}_b = \frac{k_b}{\chi R_o^2} = \frac{1}{12\left(1-\nu^2\right)}\left(\frac{h}{R_o}\right)^2;\ \hat{P}_A = \frac{P_A R_o}{\chi}}$$

Unknowns:

$r(\xi)$, $\theta(\xi)$, P_G, P_{ext}

[Barthès-Biesel et al., *J. Fluid Mech.*, 2002]

[Pozrikidis, *Modeling and Simulation of Capsules and Biological Cells*. 2003: Taylor & Francis]

[Tsiglifis & Pelekasis, *Phys. Fluids*, 2011]

[Updike & Kalnins, *Trans. ASME*, 1970, 1972, 1972]

Continuation of the solution

Simple Continuation:

$$\lambda^{N+1} = \lambda^{N} + \Delta\lambda$$

Initial guess for the

new solution (N+1): $\vec{c}^{\,N+1} = \vec{c}^{\,N}$

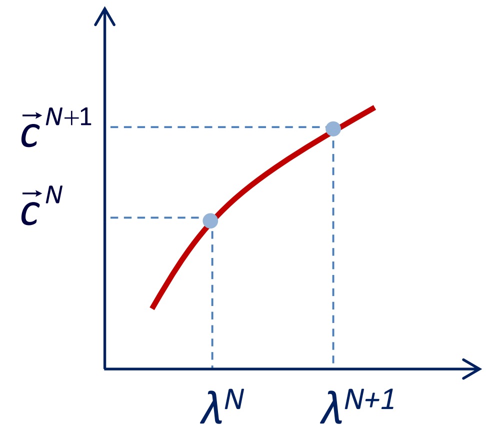

Arc-Length Continuation:

$$\begin{bmatrix} [J] & \vec{R}_\lambda \\ \vec{N}_c & N_\lambda \end{bmatrix} \begin{bmatrix} \vec{c} \\ \lambda \end{bmatrix} = \begin{bmatrix} \vec{R} \\ N \end{bmatrix} \quad \text{and} \quad \begin{bmatrix} [J] & \vec{R}_\lambda \\ \vec{N}_c & N_\lambda \end{bmatrix} \begin{bmatrix} \partial\vec{c}/\partial s \\ \partial\lambda/\partial s \end{bmatrix} = \begin{bmatrix} \partial\vec{R}/\partial s \\ \partial N/\partial s \end{bmatrix}$$

$$N = \left(c_i^{N+1} - c_i^{N}\right)^2 + \left(\lambda^{N+1} - \lambda^{N}\right)^2 - \Delta s^2$$

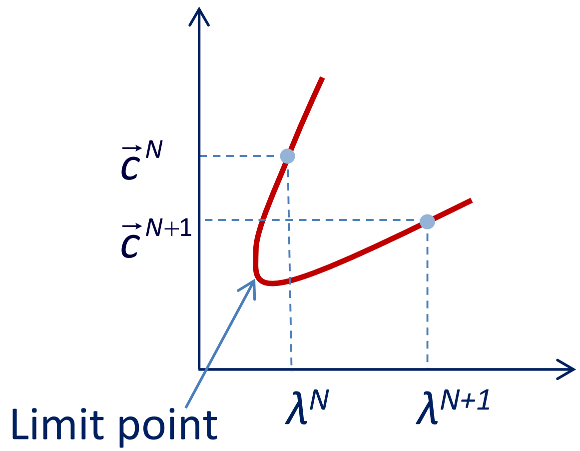

Initial guess for the new solution (N+1):

$$\vec{c}^{\,N+1} = \vec{c}^{\,N} - \frac{\partial\vec{c}^{\,N}}{\partial s}\Delta s$$

$$\lambda^{N+1} = \lambda^{N} - \frac{\partial\lambda^{N}}{\partial s}\Delta s$$

Initial Guess → Newton-Raphson Iterations → Convergence

Finite Elements-Weak Form

Weak Form-Classic contact problem

$$R_1 = \int_0^1 \left[\left(k_s \tau_{ss} + k_\varphi \tau_{\varphi\varphi} + 2k_m \sigma + P(\xi) + P_{atm} - P_G \right) B_i r \sin\vartheta s_\xi - \frac{\sigma\left(B_{i,\xi\xi} s_\xi - B_{i,\xi} s_{\xi\xi}\right)}{s_\xi^2} - \frac{m_\varphi B_{i,\xi} \sigma_\xi}{s_\xi} \right] d\xi + M_{BT}$$

$$R_2 = \int_0^1 \left[\tau_{ss} B_{i,\xi} \sigma + B_i \sigma_\xi \tau_{\varphi\varphi} + \sigma m_s \left(k_{s,\xi} B_i + k_s B_{i,\xi} \right) + k_s m_\varphi B_i \sigma_\xi \right] d\xi + N_{BT}$$

$$R_3 = P_G V^\gamma - P_{atm} V_0^\gamma$$

where

$$\xi = 0 : (\vartheta = 0) \quad M_{BT} = 0 \text{ and } N_{BT} = 0$$

$$\xi = 1 : \left(\vartheta = \frac{\pi}{2} \right) \quad M_{BT} = \frac{\sigma m_s B_{i,\xi}}{s_\xi} - \sigma q B_i \quad \textit{and}$$

$$N_{BT} = -\left[k_s m_s + \tau_{ss} \right] \sigma B_i$$

$$s_\xi = \frac{ds}{d\xi} = \sqrt{r^2 \vartheta_\xi^2 + r_\xi^2} \;;\; \sigma = r \sin\vartheta \;;\; \sigma_\xi = \frac{d\sigma}{d\xi} = r_\xi \sin\vartheta + r\vartheta_\xi \cos\vartheta$$

Validation of Bifurcation Diagrams

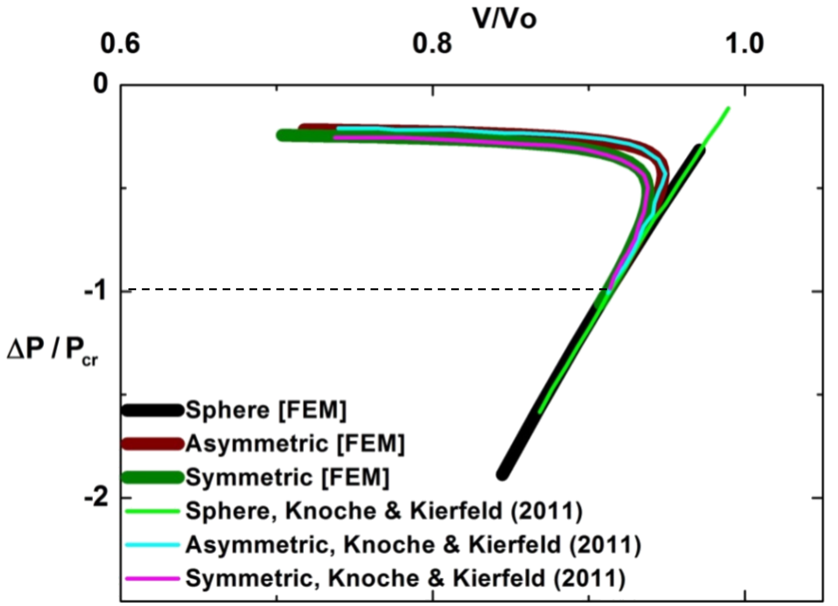

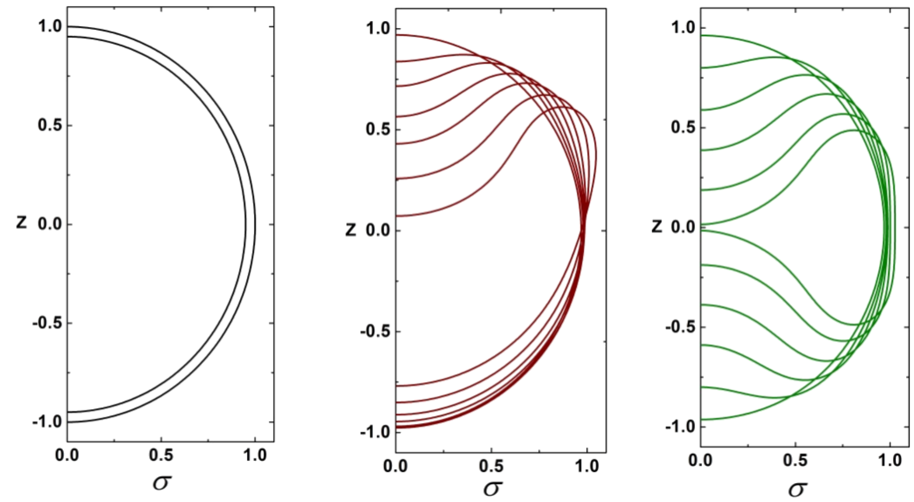

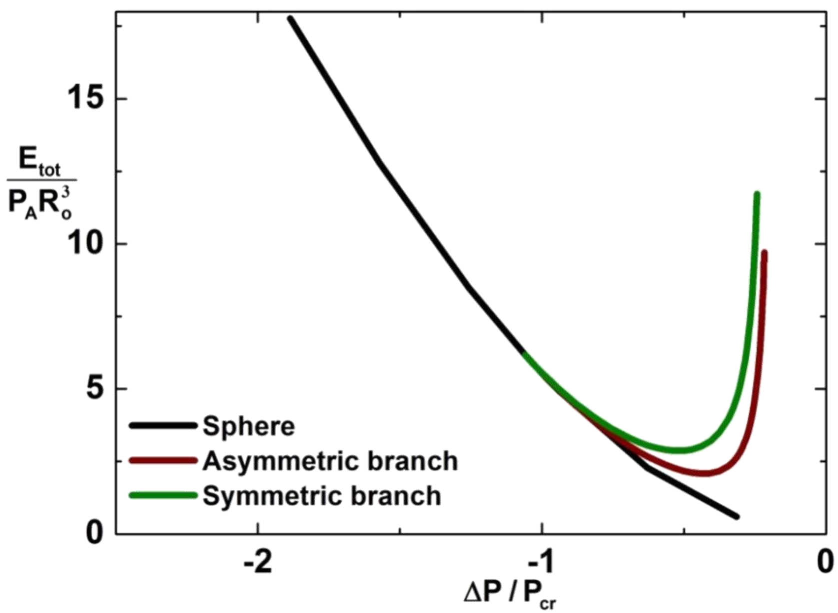

$\hat{k}_b = 10^{-3}, \hat{P}_A = 4\cdot 10^{-3}$

$E = 2.64\cdot 10^{8}\, Pa, h = 1.9\cdot 10^{-7}\, m, R_o = 2\cdot 10^{-6}\, m$

$\nu = 0.5, \gamma_{BW} = 0\ N/m, \gamma = 1.07$, Hook's law, $u = 0$

[Knoche & Kierfeld, *Physical Review E*, 2011]

Parametric Study: $\hat{P}_A << 1$ Microbubbles covered with polymer: ***Effect of adhesion***

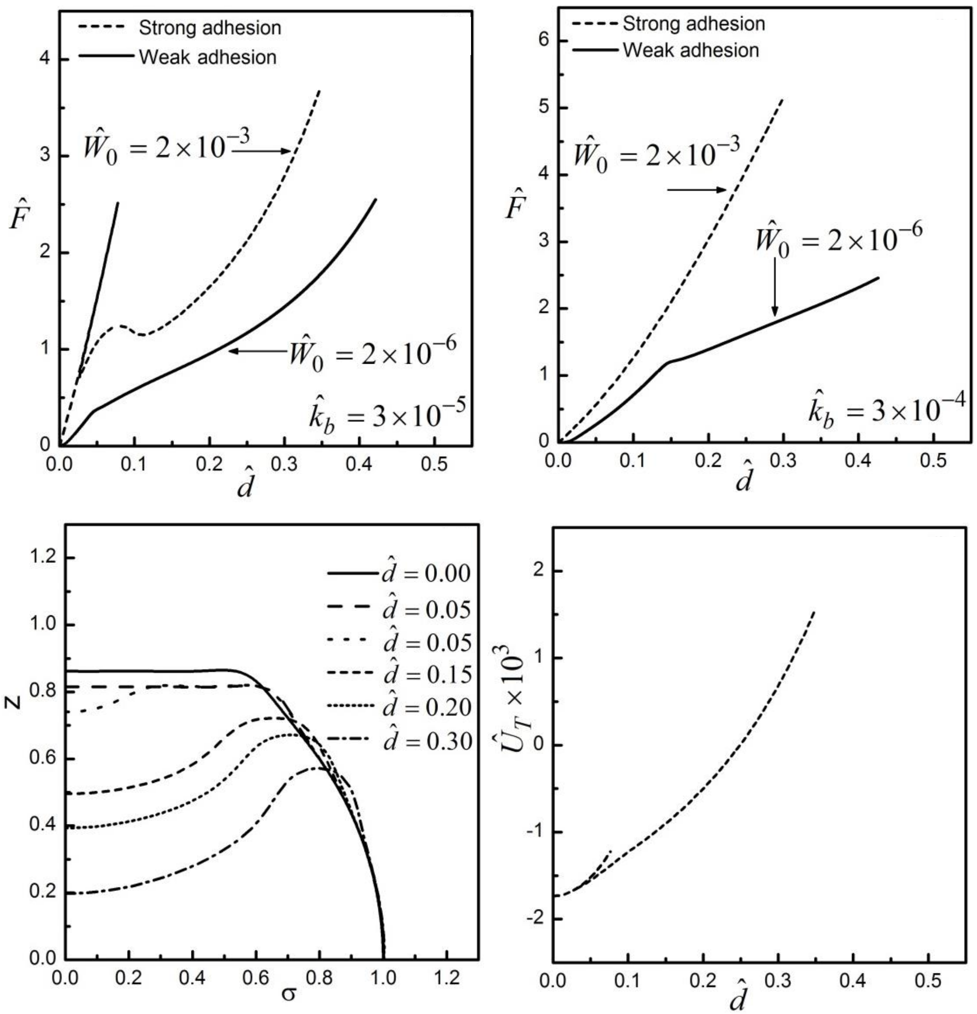

$\hat{k}_b = 3\times10^{-5}$, $\hat{P}_A = 3\times10^{-5}$, $\hat{W}_0 = 2\times10^{-3}$, $\hat{\gamma}_{BW} = 0$
$\nu = 0.5$, $\gamma = 0$, *Hooke's law*, $\mathrm{u} = 0$

- Buckling is postponed or even by-passed as adhesion increases.
- When strong adhesion is considered, the zero point force does not correspond to an undeformed shape.
- The flat solution after the buckling point has higher energy: Unstable branch.

[Lytra & Pelekasis, *Phys. of Fluids*, 2018]

Parametric Study: $\hat{P}_A \sim 1$ Microbubbles covered with phospholipid: ***Effect of adhesion***

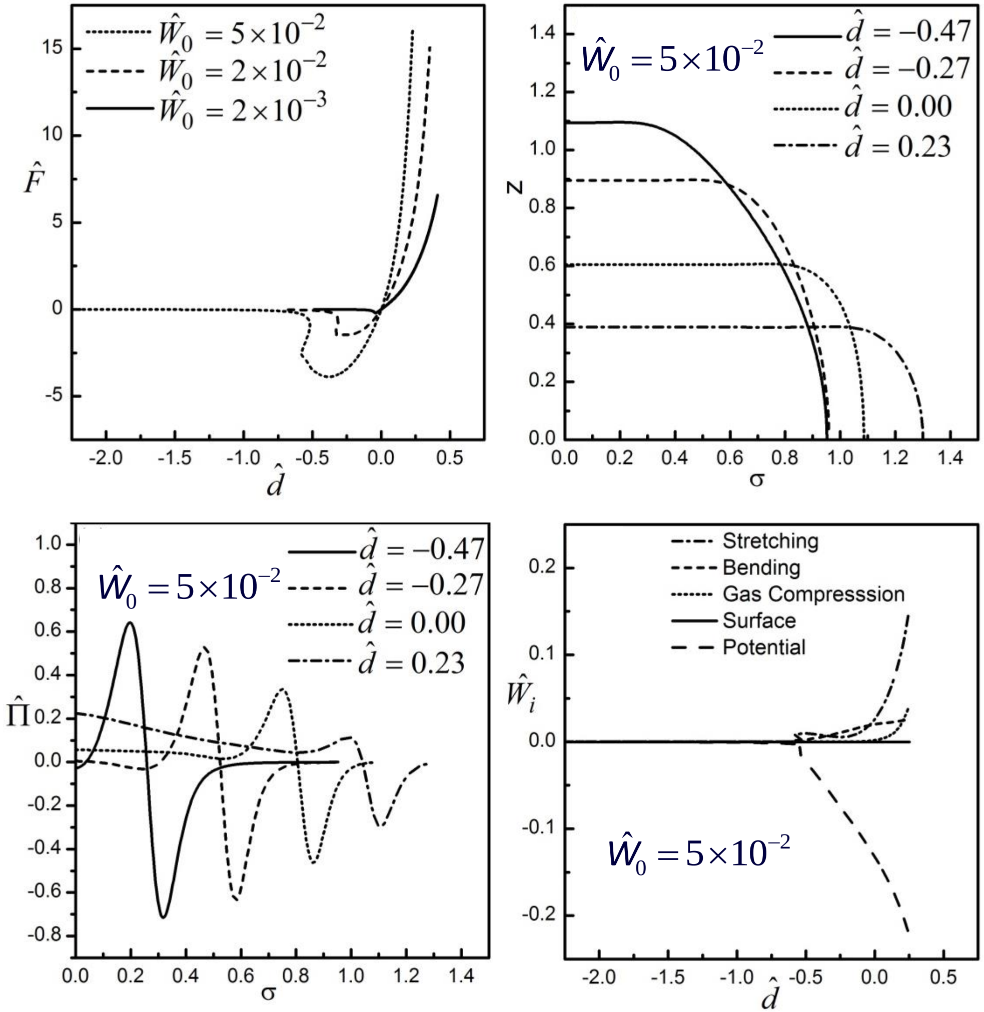

$$\hat{k}_b = 2.7\times10^{-3},\ \hat{P}_A = 3,\ \hat{\gamma}_{BW} = 0$$
$$\nu = 0.5,\ \gamma = 0,\ Mooney - Rivlin\ law,\ \mathrm{u} = 0$$

- As the adhesion parameter increases both repulsive and maximum attractive forces increase.
- The shape of the shell at maximum attraction is significantly deformed with the position of the pole at a value higher than the initial.
- The competition between the thinning of the liquid film and the increase of the gas pressure results an increase in in-plane stresses.
- The latter generate a linear response in f-d curve with slope higher than Reissner slope.

[Lytra & Pelekasis, *Phys. of Fluids*, 2018]